Response of the benthic nepheloid layer to near-inertial internal waves in southern Lake Michigan

Nathan Hawley

Great Lakes Environmental Research Laboratory, Ann Arbor, Michigan, USA

Received 18 September 2003; revised 15 January 2004; accepted 27 February 2004; published 7 April 2004.

[1] Time series measurements of water transparency, water temperature, and current velocity were made at a station located in 58 m of water in southern Lake Michigan during the summer of 1995. Currents generated by near-inertial internal waves are correlated with variations in the thickness and in the vertical distribution of suspended sediment in the benthic nepheloid layer. Although a direct causal link between internal wave action and changes in the nepheloid layer could not be established, the data suggest that local resuspension by shoaling internal waves maintains the layer during the stratified period. The origin and maintenance of the benthic nepheloid layer is most likely the result of local resuspension due to a combination of internal wave action and longer-term processes. *INDEX TERMS:* 4558 Oceanography: Physical: Sediment transport; 4544 Oceanography: Physical: Internal and inertial waves; 4239 Oceanography: General: Limnology; *KEYWORDS:* Lake Michigan, nepheloid layer, sediment resuspension, Morlet wavelet

Citation: Hawley, N. (2004), Response of the benthic nepheloid layer to near-inertial internal waves in southern Lake Michigan, *J. Geophys. Res.*, *109*, C04007, doi:10.1029/2003JC002128.

1. Introduction

[2] Nepheloid layers are a common feature in both large lakes and the world's oceans. The layers are identified by either acoustic or optical measurements and are caused primarily by increased concentrations of material suspended in the water column. Benthic nepheloid layers (bnl) are defined as extending upward from the bottom until a minimum attenuation is reached in the middle of the water column [*McCave*, 1986]. Intermediate nepheloid layers (inl, which usually occur at or near pycnoclines) and surface nepheloid layers (snl) have also been identified.

[3] In the oceans, benthic nepheloid layers are usually presumed to be due to local resuspension of bottom sediments. *Cacchione and Drake* [1986] suggested that some bnls could be created by the shoaling and breaking of internal waves on the continental shelf. This hypothesis is supported by both field observations [*Bogucki et al.*, 1997; *Johnson et al.*, 2001; *Puig et al.*, 2001] and by numerical investigations [*Ribbe and Holloway*, 2001; *Wang et al.*, 2001].

[4] In Lake Michigan the bnl is almost always present in the hypolimnion during the stratified period and is also found to a lesser degree during the unstratified period. Vertical profiles of water temperature and beam attenuation made in the southern basin of the lake in 1983 (N. Hawley, unpublished data) at stations in water depths between 50 m and 150 m show the presence of the bnl at all stations throughout the stratified period. *Sandilands and Mudroch* [1983] found a similar occurrence of the bnl in Lake Ontario. Observations made during the unstratified period [*Hawley and Lee*, 1999; N. Hawley, unpublished data) show that the bnl is far less well developed during the unstratified period except during and immediately after storms. Since near-inertial internal waves are a prominent feature of the offshore circulation during the stratified period [*Mortimer*, 1980], and since they do not exist when the lake is unstratified, it is possible that the formation and maintenance of the bnl is related to the presence of these waves.

[5] The first investigation of the bnl in the Great Lakes was by *Chambers and Eadie* [1981], who speculated that it was caused by local resuspension caused by "the rubbing of the thermocline across the bottom." Since then, several subsequent investigators have proposed theories for the origin and maintenance of the bnl in the Great Lakes. These include local resuspension [*Chambers and Eadie*, 1981; *Sandilands and Mudroch*, 1983; *Rosa*, 1985; *Baker and Eisenreich*, 1989; *Halfman and Johnson*, 1989; *Mudroch and Mudroch*, 1992], downslope advection of nearshore material [*Halfman and Johnson*, 1989], and settling of biogenic material [*Sly*, 1994]. Although time series measurements of both current velocity and water transparency are required to test these hypotheses, none were made in any of these studies.

[6] Recently, however, the results of several such time series studies have been reported. *Hawley and Lesht* [1995] analyzed several months of time series observations in Lake Michigan in water depths of 65–100 m and found no instances of bottom resuspension. They suggested that the bnl was maintained by a combination of vertical mixing and the offshore transport of material during downwelling events. Although Hawley and Lesht speculated that internal wave action supplied at least some of the energy for vertical mixing, their data were insufficient to document their speculation. *Hawley and Murthy* [1995] found no evidence

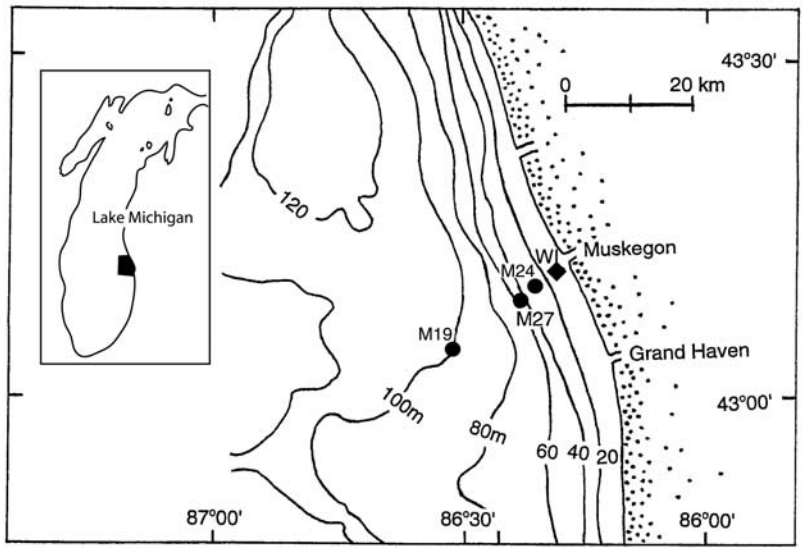

Figure 1. Location map showing the position of the three mooring sites. The water depths were 28 m at M24, 58 m at M27, and 100 m at M19. WI denotes the position of the Muskegon water intake, where data were also collected.

of either resuspension or downslope transport during a downwelling event in Lake Ontario. *Lee and Hawley* [1998] examined the effects of upwelling and downwelling events on the bnl in Lake Michigan. They too found that material was not directly supplied to the bnl during downwelling events. Although near-inertial internal waves are evident in the initial part of their observations, they did not discuss their effects. In all of these studies, variations in both the thickness of the bnl and the concentration of material suspended within it were observed, but no obvious physical forcing was identified.

[7] More recently, *Hawley and Muzzi* [2003] described changes in attenuation and temperature recorded by a moored vertical profiler. They observed changes in the bnl due to near-inertial internal waves and found that episodes of high bottom turbidity coincided with periods when the thermocline was elevated. Hawley and Muzzi determined that the total amount of material suspended in the bnl changed with time and (although no velocity measurements were made) speculated that the high turbidity episodes were caused either directly or indirectly by the shoaling of near-inertial internal waves on the lake slope.

2. Site Description and Methods

[8] Instrumented tripods were deployed at three stations in southern Lake Michigan during the summer of 1995 as part of the EPA's Lake Michigan Mass Balance Program. The stations were located in water depths of 28 m (M24, 5 km offshore), 58 m (M27, 10 km offshore), and 100 m (M19, 28 km offshore) along a transect that originated in Muskegon, Michigan, and ran roughly perpendicular to the shoreline (Figure 1). Since this investigation concentrates on the results from M27, only those observations are described here; a full description of all of the observations and a preliminary interpretation is given by *Hawley* [2003]. M27 is one of the sites described by *Lee and Hawley* [1998], and is located very close to the site where *Hawley and Muzzi* [2003] made their observations. The site is located near the edge of the coastal boundary layer [*Murthy and Dunbar*, 1981], so the effects of both upwellings/downwellings and near-inertial internal waves could be important. These waves have periods slightly less than the inertial period of the lake (17.6 hours), and have circular particle trajectories about 1 km in diameter [*Mortimer*, 1980]. An instrumented mooring was deployed at the site (43°10.14′N, 86°26.02′W) on July 11, 1995, and retrieved on August 22, 1995. Observations of water temperature and beam attenuation coefficient (bac, a measure of suspended sediment concentration) were made for 1 min each hour at 1, 7, 17, and 35 m above the bottom (mab). Vector averaging current meters on a separate mooring (located about 150 m away) recorded continuous 15-min averages at 1, 17, and 35 mab. Vertical profiles of water temperature and bac were made 13 times with a Seabird CTD unit equipped with a 25-cm Sea Tech transmissometer. Bottom material at the site is a silty sand.

[9] Bottom stresses were calculated using the method of *Li and Amos* [2001]. Spectral time series analyses were done using standard techniques. The wavelet power spectra were computed using software developed by *Torrence and Compo* [1998], the wavelet cross coherences were calculated using the algorithm presented by *Torrence and Webster* [1999]. Values were calculated each hour at 37 periods ranging from 2.2 hours to 325 hours. The interval between the periods varied logarithmically and was about 2.2 hours at 17.6 hours. The 95% confidence level for the spectral coherence was calculated using the method of *Jenkins and Watts* [1969]. The confidence levels for the wavelet cross coherences and phase angles are based on Monte Carlo simulations (20,000 simulations).

3. Observations

3.1. Vertical Profiles

[10] The profiles made at M27 (Figure 2) show that as the lake became more stratified the depth of the thermocline

(determined as the depth of the 10° isotherm) decreased from about 23 m to 12 m. This decrease was not monotonic however, and the thermocline depth could vary several meters in 1 day (July 12–13). The sensors located 1, 7, and 17 mab were always located in the hypolimnion, but the sensors 35 mab were sometimes in the thermocline. The beam attenuation measurements show a well-developed bnl in each of the profiles. The thickness of the bnl varied considerably: On some days it occupied the entire hypolimnion (July 17), while on other days it was confined to a fairly thin layer near the bottom (July 21). The bac decreased with increasing height above the bottom, but the shape of the profile varied from day to day. The maximum attenuation in the bnl varied between 3 and 6 m^{-1}, while the minimum attenuation above the bnl was approximately 0.65 m^{-1}. The minimum value in each profile was used to determine the thickness of the bnl on that day. The attenuation measurements in the bnl were converted to the concentration of suspended material using the equation of *Hawley and Zyren* [1990]. Table 1 shows the thickness of the bnl, the amount of suspended material in a 1-m^2 column extending through the bnl, and the average concentration of material in the bnl. These calculations show that both the thickness of the bnl and the amount of material suspended within it could vary by more than a factor of 2 within a few days.

[11] Many of the profiles also show an inl near the base of the thermocline. This layer is most noticeable at the end of the deployment. The observations at 35 mab were usually made in the clearer water between the bnl and the inl, while the observations made at the lower elevations were usually made within the bnl. However, on several occasions the 17 mab observations were made either above or very near the top of the bnl, and on July 17 the 35 mab observations were within the bnl.

3.2. Time Series Observations

[12] Winds during the deployment were light (less than 10 m/s) and varied in direction (Figure 3). The light winds produced relatively small waves during the deployment. Maximum wave heights and periods recorded by NDBO buoy 45007 (located in the center of the southern basin about 70 km to the southwest) were about 2 m and 6.5 s. The effects of these waves did not reach the bottom at M27, but the maximum stress due to the currents alone was 0.07 Pascals. This value is considerably below the threshold required for sediment movement (0.13 Pascals). Currents at the three elevations at M27 (Figure 3) were quite similar to each other, although the rotary motions due to near-inertial waves are more pronounced at the upper elevations. The near-inertial motions dominate the circulation on July 17–22 and are also important between July 28 and August 12. These intervals are probably the result of the modification of the long-term currents by the upwelling events that occurred during the deployment (upwellings on July 18–19, August 1–4, and August 7–9 can be seen in the temperature records at M24 [*Hawley*, 2003]. These two intervals divide the current record into five parts, with relatively strong alongshore flow during the other three periods (July 11–17, July 22–28, and August 12–22). This alongshore motion is much more pronounced than at either M24 or M19.

[13] The most noticeable feature of the time series measurements at M27 (Figure 4) are the numerous short-period oscillations in the records. The hourly sampling interval and relatively short deployment time prohibits the distinction between inertial and near-inertial periods in a power spectra analysis of the data, so the term "inertial period" is used here to denote characteristics of the spectra at or near the inertial period. The power spectra analyses (Figure 5) show peaks in the energy spectra at the inertial period (17.6 hours) for all of the parameters except the 1 mab attenuation, so the short-period oscillations are probably due to the passage of near-inertial waves. The effects of upwellings are evident in the decreases in the 35 mab temperature on July 18 and August 1. Temperatures at the other three elevations are much lower and show little change throughout the deployment.

[14] The attenuation measurements show considerable variation at both the inertial period and on a longer timescale. The long term variations in the attenuations at the two lowest elevations are very similar to each other. Both have their highest values (July 18 and August 5) during intervals when the currents were weak, and show a gradual decline after August 12. The 17 mab observations are similar to those at the lower elevations, but there are two intervals (July 20–23 and August 3–4) when the attenuation is both very low and relatively constant. These are periods when the thickness of the bnl was less than the elevation of the sensor. The vertical profile made on July 21 confirms that the bnl was only 12 m thick on that day. Immediately before and after these intervals the attenuation varied greatly; these are periods when the top of the bnl oscillated up and down past the sensor. At other times during the deployment (July 14–20, July 28 to August 2, August 5–8, and August 12–23) the bnl was over 17 m thick. The top of the bnl moved up and down past the 7 mab sensor on July 20–23 and August 3–4, so the thickness of the bnl varied from less than 7 m to over 35 m (on July 17) during the observation period. The variations in the 35 mab attenuation are much less than at the lower elevations and show little relationship to them. These variations are due to movement of the inl as the thermocline moves up and down in the water column [*Hawley and Muzzi*, 2003; *Hawley*, 2003]. Since the analysis is concerned only with the bnl, the 35 mab observations will not be discussed further.

[15] Scatterplots show that the current velocity components at the different depths are very similar to each other, but this is not true for either the temperatures or the attenuations. Nor is there any consistent relationship between the attenuation and the other parameters at a given depth (Figure 6). Correlation coefficients based on linear regressions for different pairs of parameters show that the current speeds and velocity components at different elevations are highly correlated, but there is little correlation between either the temperatures or the attenuations at different elevations, or between the attenuation and any of the other parameters at a given depth. The spectral coherences between the same parameter at different elevations are somewhat higher than the correlation coefficients, but they are only significantly different from zero for the current speeds and the velocity components, and between the near-bottom (1 and 7 mab) temperatures. Nor are the coherences

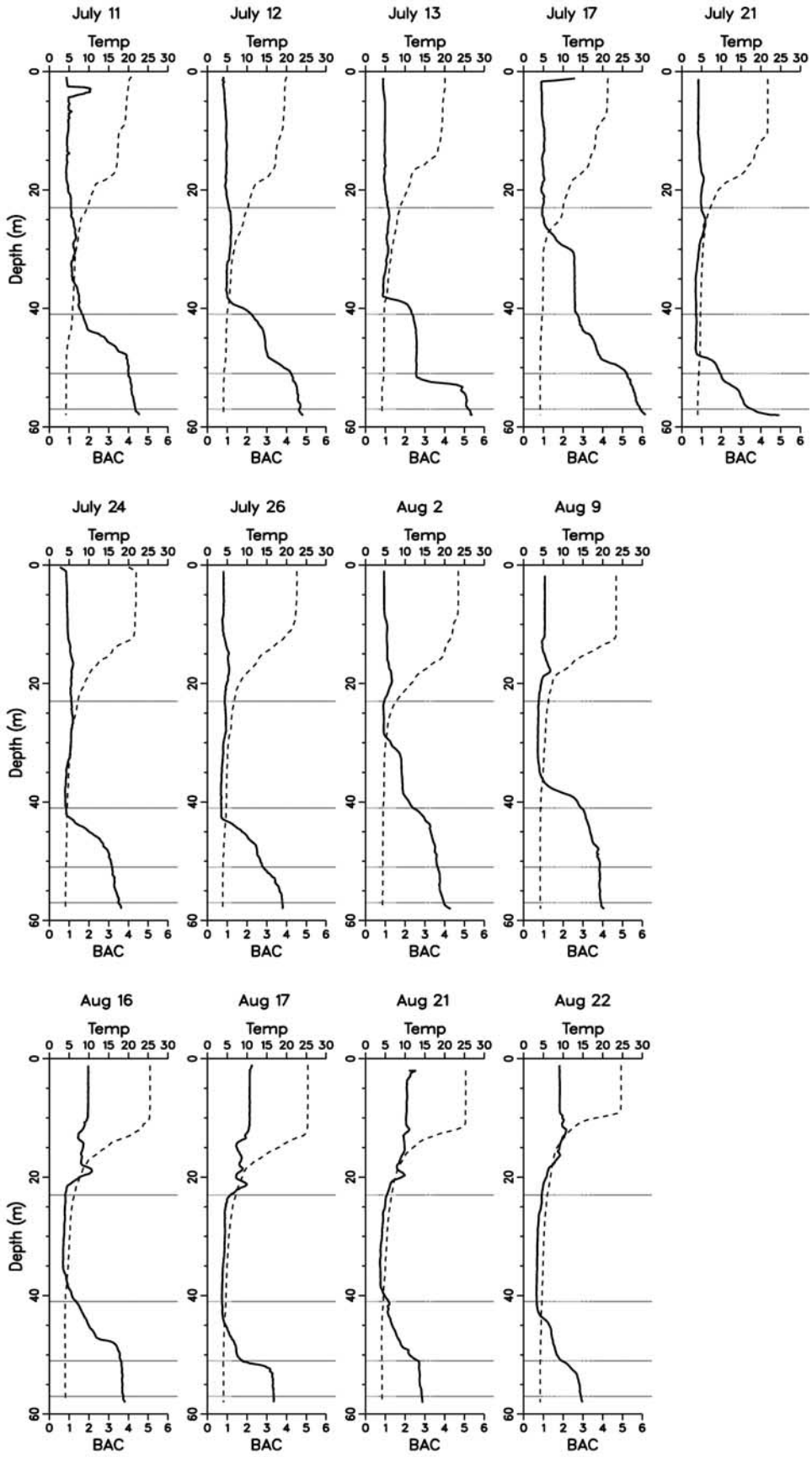

Figure 2. Data from the vertical profiles at M27. The solid line is the bac (1/m), and the dashed line is the temperature (°C). Heights of the time series observations are shown by the horizontal lines.

Table 1. Thickness of the bnl (m), the Total Suspended Material (g) in a Vertical 1 m^2 Column Extending Through the bnl, and the Average Concentration (g/m^3) at M27

Date	M27 BNL Thickness	M27 Total Material	M27 Average Concentration
July 11	26	134	5.4
July 12	22	140	6.4
July 13	22	128	5.8
July 17	39	244	6.3
July 21	12	49	4.1
July 24	21	91	4.3
July 26	20	87	4.4
August 2	35	160	4.6
August 9	29	146	5.0
August 16	21	110	5.2
August 17	22	65	3.0
August 21	24	73	3.0
August 22	19	58	3.1

between the beam attenuation and the other parameters at the same depth significantly different from zero.

3.3. Wavelet Analysis

[16] Nepheloid layers are well developed at the station and occurred throughout the stratified period (the layers are present in all vertical profiles made between the time stratification began in early May and ended in late October). This indicates that conditions during the stratified period are favorable in some way for the development and maintenance of these layers. The peaks in the power spectra suggest that near-inertial wave action is somehow related to the occurrence of the layers, but the analysis so far shows no significant correlation between near-inertial motions in either the currents or the water temperature and the changes in bac. However, in order for the correlation coefficients to be large, or for the coherences to be significantly different

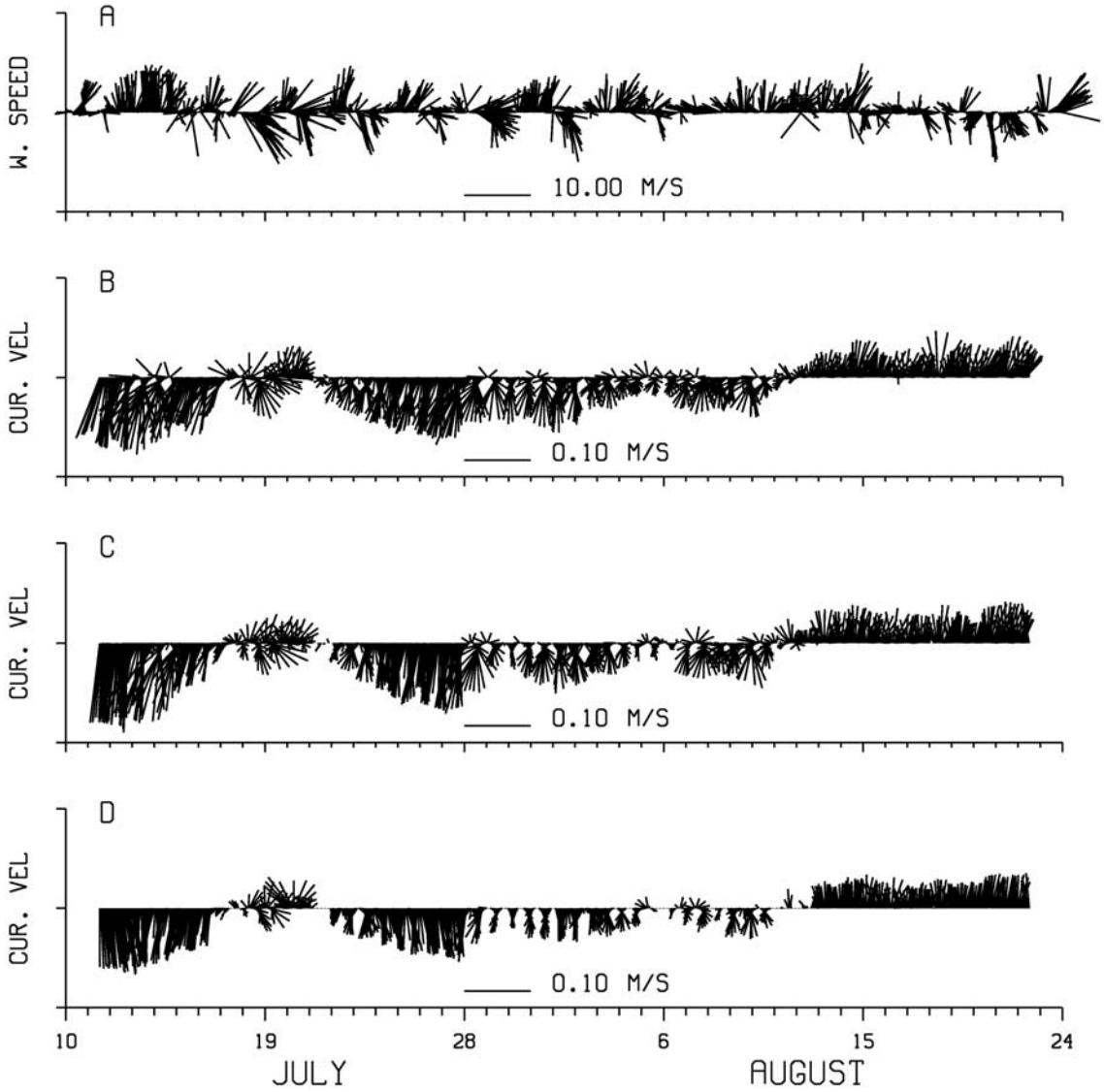

Figure 3. Winds and current velocities at M27. The currents have been rotated 37° so that up (north) and down (south) are alongshore, and offshore is to the left. (a) Wind speed at Muskegon. (b) Current velocity 35 mab at M27. (c) Current velocity 17 mab at M27. (d) Current velocity 1 mab at M27.

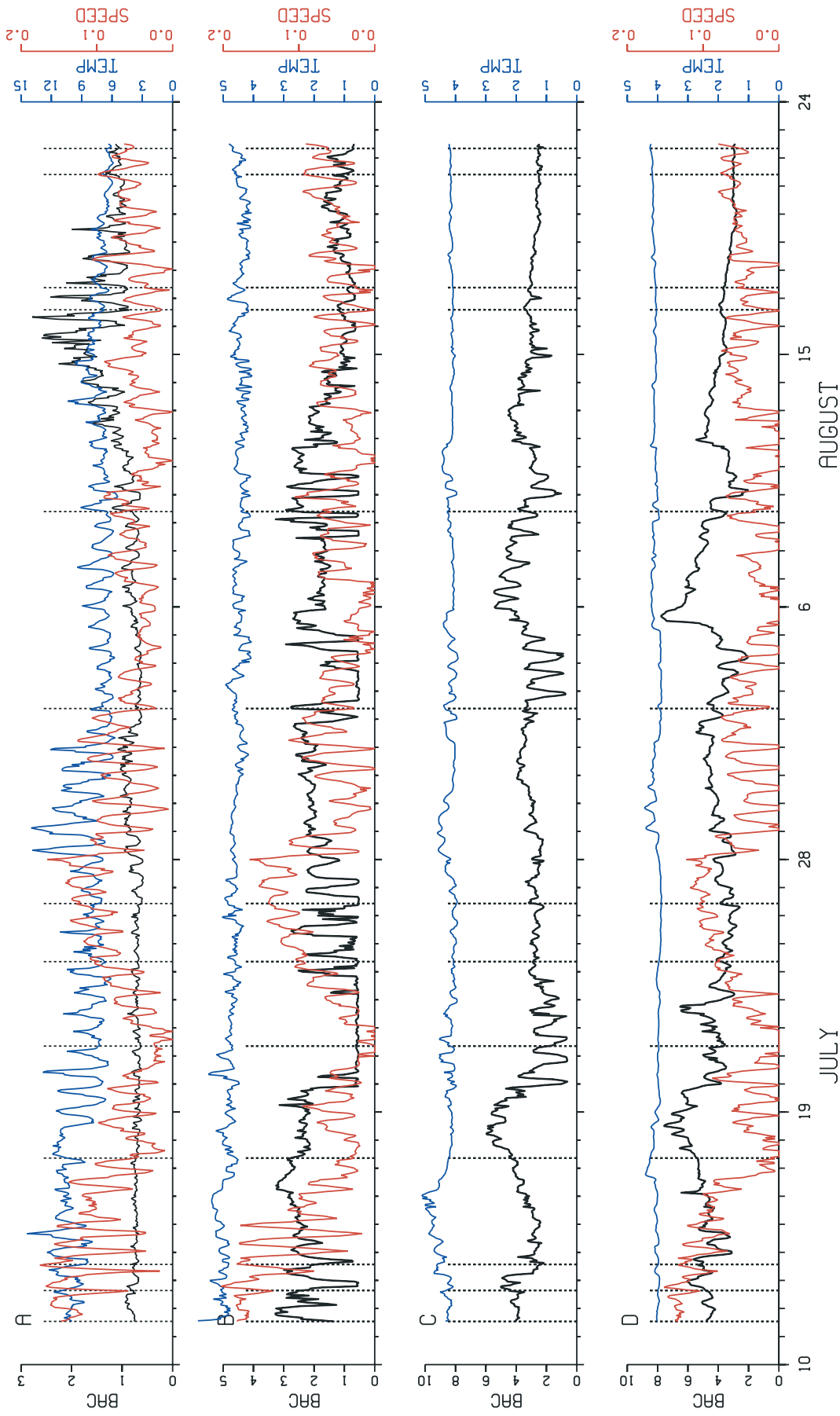

Figure 4.

from zero, the relationship between the parameters must be both linear and relatively constant with time. Since the scatterplots between bac and the other parameters show that neither of these conditions hold, it is not surprising that the correlations and the coherences are low. It would be more useful to identify periods within the observation period when the relationship between the various parameter pairs is relatively constant, and then determine the relationship during those intervals.

[17] Wavelet analysis is a relatively recent development in time series analysis that facilitates such an approach. Its chief advantage over Fourier analysis is that it allows one to characterize the energy distribution of a parameter as a function of both time and period (or frequency). Since the analysis is sensitive to changes in the observed parameters it is highly suitable for the analysis of events that occur during only a small fraction of the observation period. The Morlet wavelet is used here; this wavelet has been used in several previous environmental studies [*Meyers et al.*, 1993; *Liu and Miller*, 1996; *Torrence and Webster*, 1999] because it is relatively easy to interpret, and because it offers fairly good resolution in both time and period. The analysis below uses wavelets to identify intervals in the records when near-inertial wave action was most pronounced, and to determine if a consistent relationship between the attenuation and the other parameters exists during these intervals.

[18] Figure 7 shows the wavelet power spectra for the observed parameters at M27 as a function of period (in hours) and time. The contours are multiples of the energy level that is significantly different from zero at the 95% confidence level when compared to a white noise spectra [*Torrence and Compo*, 1998]. The energy in the wavelet power spectra is concentrated in two distinct bands: one at periods greater than about 100 hours and the second centered around the inertial period. The time intervals when the energy at the inertial period is significant are more continuous for the cross-shore velocities than for the alongshore velocities because the long-term currents are primarily alongshore. The distribution over time of the longer-period energy is somewhat misleading since edge effects affect the values of the wavelet coefficients at the beginning and end of the observation interval. This effect is significant over about 2 times the period for which the wavelet coefficients are calculated (the cone of influence [*Weng and Lau*, 1994]), so although the general observation that there is considerable energy at the longer periods is undoubtedly correct, it would be risky to say too much about the distribution of energy with time for periods greater than 100 hours.

[19] Significant energy concentrations at the inertial period are present in the spectra for the attenuations at both 7 and 17 mab during the intervals when the attenuations vary most (Figures 7d and 7f), and the wavelet spectrum also shows that there are several intervals when even the 1 mab beam attenuation varies at the inertial period (Figure 7h). These results indicate that changes in the attenuations at all elevations are at least partly due to near-inertial wave action, but that longer-term processes are also important. The temperature spectra show some intervals where the energy is significant, but since the changes in temperature are so small, it is unlikely that they are important.

[20] The wavelet cross coherence [*Torrence and Webster*, 1999] measures the degree that two parameters covary as a function of both time and period; as such, it is analogous to the classic bivariate coherence (which measures how well two parameters covary at a given period over the entire observation interval). The cross coherence may be high even when the wavelet power spectra for the individual parameters are low; this indicates that a relationship exists between the parameters even when the parameters do not vary too much. The wavelet phase angle is also analogous to that in classical time series analysis, but it determines the phase angle as a function of both time and period. The wavelet cross coherences between the velocity components show that at the inertial period, the velocity components at both elevations are strongly covarying at virtually all times during the deployment (not shown). The phase angle at the inertial period between the velocity components at each elevation is 90°, as would be expected since the water motion due to near-inertial waves is nearly circular. The cross coherences between both the temperatures and the attenuations measured at different elevations are far less consistent. For the temperatures at least, this is because the temperature variations at the lower three elevations are so small.

[21] The cross coherence between the 1 and 7 mab attenuations is greatest at periods longer than about 50 hours (Figure 8), but there is little cross coherence at the inertial period. In fact, the cross coherence is greater at periods shorter than the inertial period. This may indicate that the actual mechanism for causing the changes in bac occurs at periods somewhat shorter than the inertial period, or it may be that, since there is little energy at these shorter periods for either of the attenuations, the result is unimportant. The variations in the two attenuations at the inertial period are roughly in phase during most of the intervals when the cross coherence is significantly different from zero. The cross coherences between the 17 mab attenuation and both the 1 and 7 mab attenuations are more focused at the inertial period, and the phase angles show that the 17 mab attenuation is either essentially in phase, or essentially out of phase, with the near-bottom attenuations during these intervals.

[22] The cross coherence between the 1 mab attenuation and both the speed and the temperature is almost never significant, but the cross coherence between the

Figure 4. Time series measurements at M27. The colors of the axes correspond to the colors of the observations. The dotted vertical lines indicate the times of the vertical profiles shown in Figure 2. (a) The beam attenuation (black, 1/m), temperature (blue, °C), and current speed (red, m/s) 35 mab. (b) The beam attenuation (black, 1/m), temperature (blue, °C), and current speed (red, m/s) 17 mab. (c) The beam attenuation (black, 1/m) and temperature (blue, °C) at 7 mab. No current measurements were made at this elevation. (d) The beam attenuation (black, 1/m), temperature (blue, °C), and current speed (red, m/s) at 1 mab.

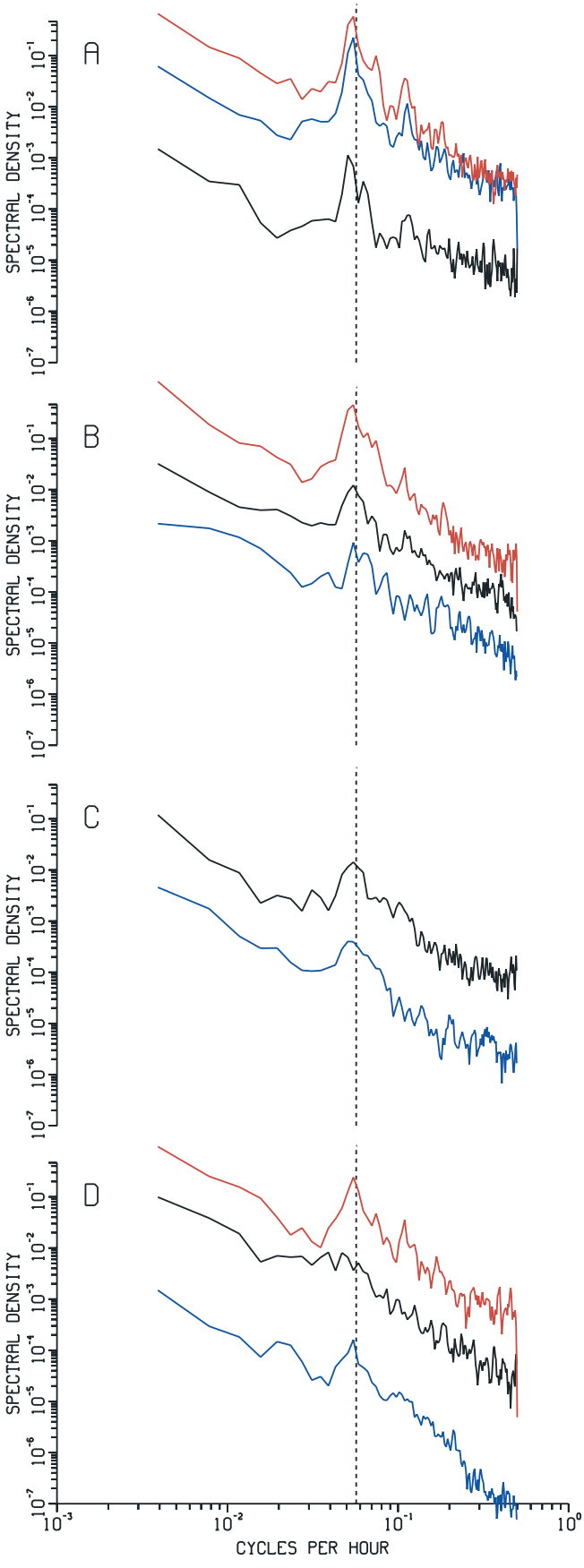

attenuation and the cross-shore velocity is significant during several intervals (Figure 9). The intervals of high cross coherence tend to be centered at periods equal to or slightly less than the inertial period. During the intervals when the cross coherence at the inertial period is significant, the phase angle between the attenuation and the cross-shore velocity varies, but during the three intervals that occur when near-inertial motions are most pronounced (July 19–21, August 2–3, and August 9–11), peaks in the cross-shore velocity lag peaks in the attenuations by between 30° and 90° (Table 2). Since the cross-shore velocity is positive when it is directed onshore, the attenuation peaks occur at times when the cross-shore velocity is increasing in the onshore direction. During the other three intervals the attenuation peaks occur when the cross-shore velocity is either directed onshore but has passed its maximum value and is slowing down (July 13–15), or the cross-shore velocity is near its maximum and directed offshore (July 25 and August 22). However, the attenuation energy during these last two intervals is not significant, so during all of the periods when the energy in both the attenuation and the cross-shore velocity is significant, and the cross coherence between the two is also significant, the inertial component of the velocity is onshore. Similar relationships are observed at both 7 mab and 17 mab.

[23] Wavelet analysis of the data collected at M24 gives results similar to those in Table 2 with one notable exception: The phase angle between the cross-shore velocity and the bottom attenuation is about 90° instead of −90° (Table 3). This means that the maximum attenuation occurred as the cross-shore velocity changed from onshore to offshore, so the onshore excursion was at its maximum extent. Near-bottom temperature changes at this station were much larger than at M27 [*Hawley*, 2003], and the phase angle between the near-bottom attenuations and the near-bottom temperatures during the events listed in Table 3 was always about 180°. Both of these results are consistent with the advection of cooler, more turbid water from farther offshore due to near-inertial wave action, followed by the offshore movement of this water as the current direction changed.

[24] At M19 the lake bottom is almost flat and there is no topographic steering of the currents [*Hawley*, 2003]. The water motion is dominated by near-inertial wave action throughout the deployment, and although the bnl does show some response to the near-inertial waves, it is not as pronounced as at the inshore stations, nor is there any consistency in the phase angle between the bottom current and 1 mab attenuation. The 1 mab attenuation is never significantly different from zero, but there are intervals when the 7, 17, and 35 mab attenuations are significant. However, there is no consistency in the phase angles between the attenuations and the current direction,

Figure 5. Power spectra of the observations at M27. The black lines are the beam attenuations, the blue lines are the temperatures, and the red lines are the current speeds. The dashed vertical line is the inertial period (17.6 hours): (a) 35 mab; (b) 17 mab; (c) 7 mab (no current measurements were made at this elevation); and (d) 1 mab.

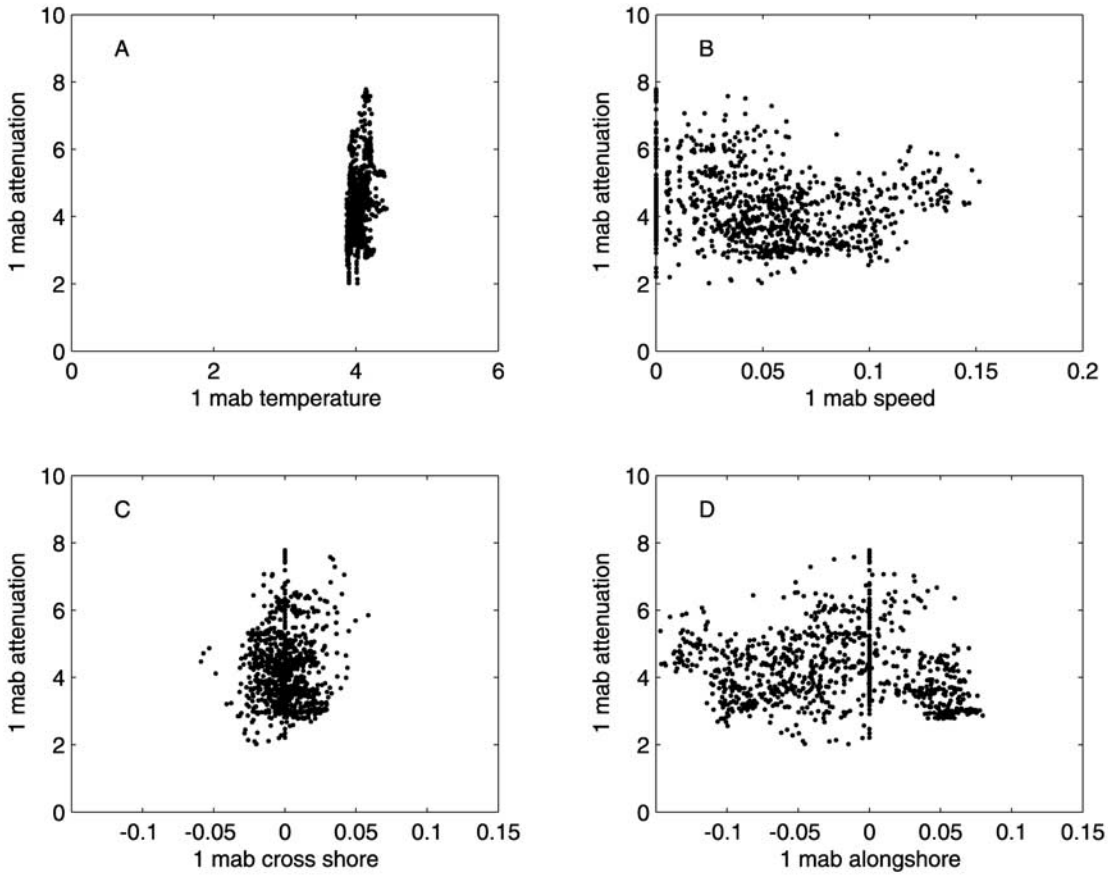

Figure 6. Scatterplots for the attenuation versus the other parameters measured 1 mab at M27. (a) Temperature and attenuation. (b) Speed and attenuation. (c) Cross-shore velocity and attenuation. (d) Alongshore velocity and attenuation.

so it is difficult to determine the cause of the increases in attenuation.

4. Discussion

[25] *Puig et al.* [2001] reported observations from a site in the Mediterranean Sea (60 m water depth) that clearly show inertial control of the suspended sediment concentration. They found a strong correspondence between increases in suspended material near the bottom and changes in the near-bottom temperature, salinity, and current direction at a period (17 hours) slightly shorter than the inertial period (18.5 hours). The increases in turbidity coincided with periods of maximum onshore velocity, so they concluded that the turbidity increases were due to the resuspension of bottom material by the shoaling and breaking of near-inertial waves on the continental slope. Puig et al. calculated that the bottom stress did not exceed 0.05 Newtons/m^2 at their site and concluded that only unconsolidated organic material could have been resuspended by the near-inertial waves. Their observations are similar to the observations reported here, so the increased turbidities observed at M27 may also be due to the resuspension of unconsolidated material by near-inertial internal waves. The maximum bottom stress due to the onshore velocity never exceeded 0.04 N/m^2, however, and since the turbidity increases occurred either prior to, or after, the time of the maximum onshore velocity, it is hard to see how resuspension by near-inertial waves could have occurred (although the data are not sufficient to completely rule out the possibility). If near-inertial waves did resuspend bottom material, then there must have been a very limited amount of material available to be resuspended at these low stresses. It is also possible that the turbidity increases are due to resuspension at or near the site by short-period (on the order of 3–10 min) internal waves. Observations of the resuspension of bottom material by such waves have been described by *Bogucki et al.* [1997] and *Johnson et al.* [2001] on the California continental shelf, and *Mortimer et al.* [1968] observed internal waves with periods of 3–10 min at a site in central Lake Michigan. If such waves occurred during the deployment, then the bottom stress could have been considerably higher for short periods of time. Unfortunately, the 15-min averaging time of the current meters used in this study makes it impossible to determine whether such waves were present. Farther inshore (at M24), the changes in attenuation are due to the onshore and offshore movement of the bnl due to near-inertial wave action. In the offshore region, changes in the bnl at the inertial period are also observed, but the cause of these changes is not evident.

[26] It is clear that while near-inertial wave action may (either directly or indirectly) cause local resuspension, resuspension does not occur all of the time. If resuspension

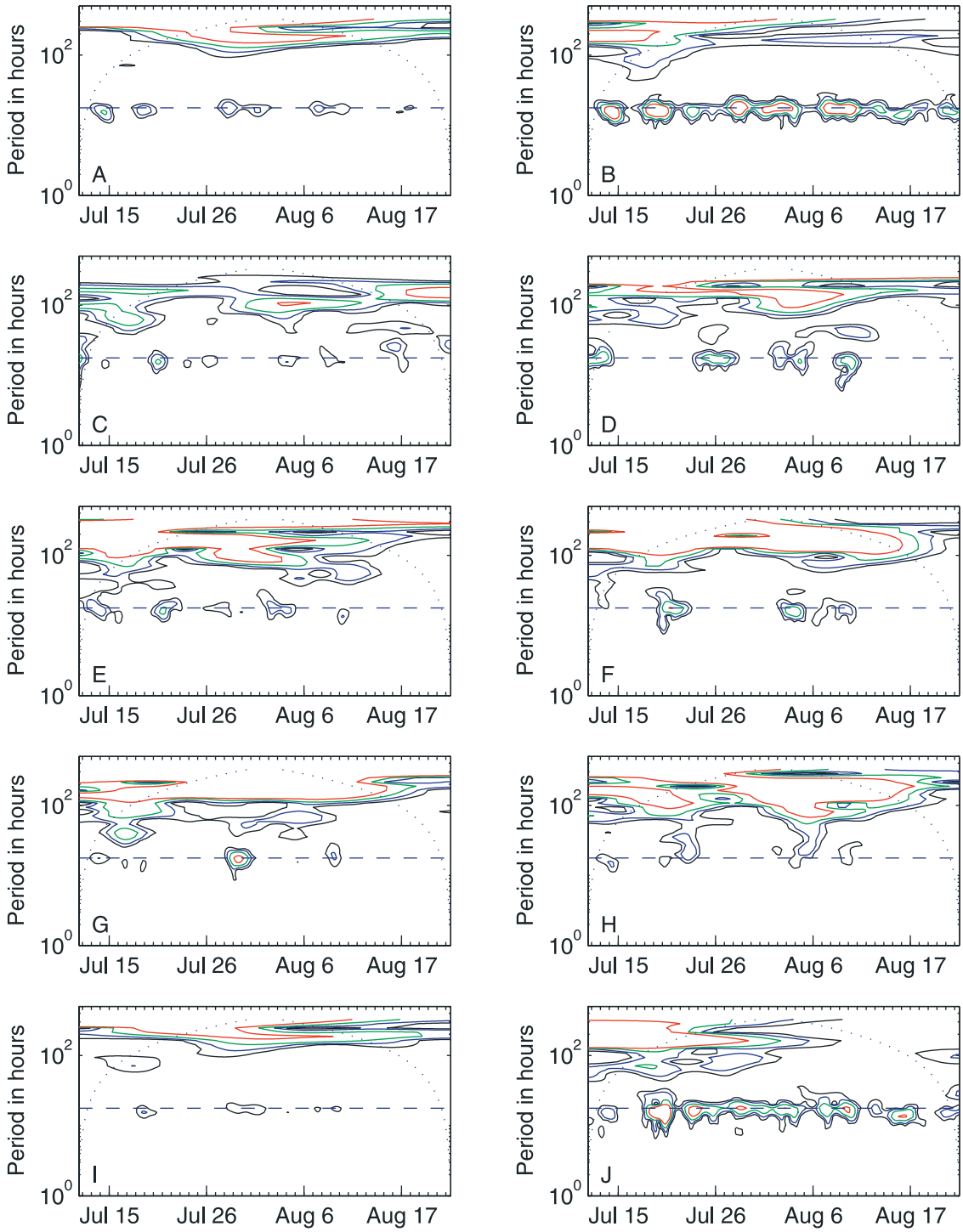

Figure 7. Wavelet power spectra for the parameters measured at M27. The black contour represents the minimum value significantly different from zero at the 95% confidence level. The other contours represent multiples of this value (2 for the blue contour, 4 for the red contour, and 8 for the green contour). The horizontal dashed line is the inertial period (17.6 h)ours. The curved dotted lines represent the cone of influence where edge effects influence the values of the power spectra. (a) Alongshore velocity at 17 mab. (b) Cross-shore velocity at 17 mab. (c) Temperature at 17 mab. (d) Attenuation at 17 mab. (e) Temperature at 7 mab. (f) Attenuation at 7 mab. (g) Temperature at 1 mab. (h) Attenuation at 1 mab. (i) Alongshore velocity at 1 mab. (j) Cross-shore velocity at 1 mab.

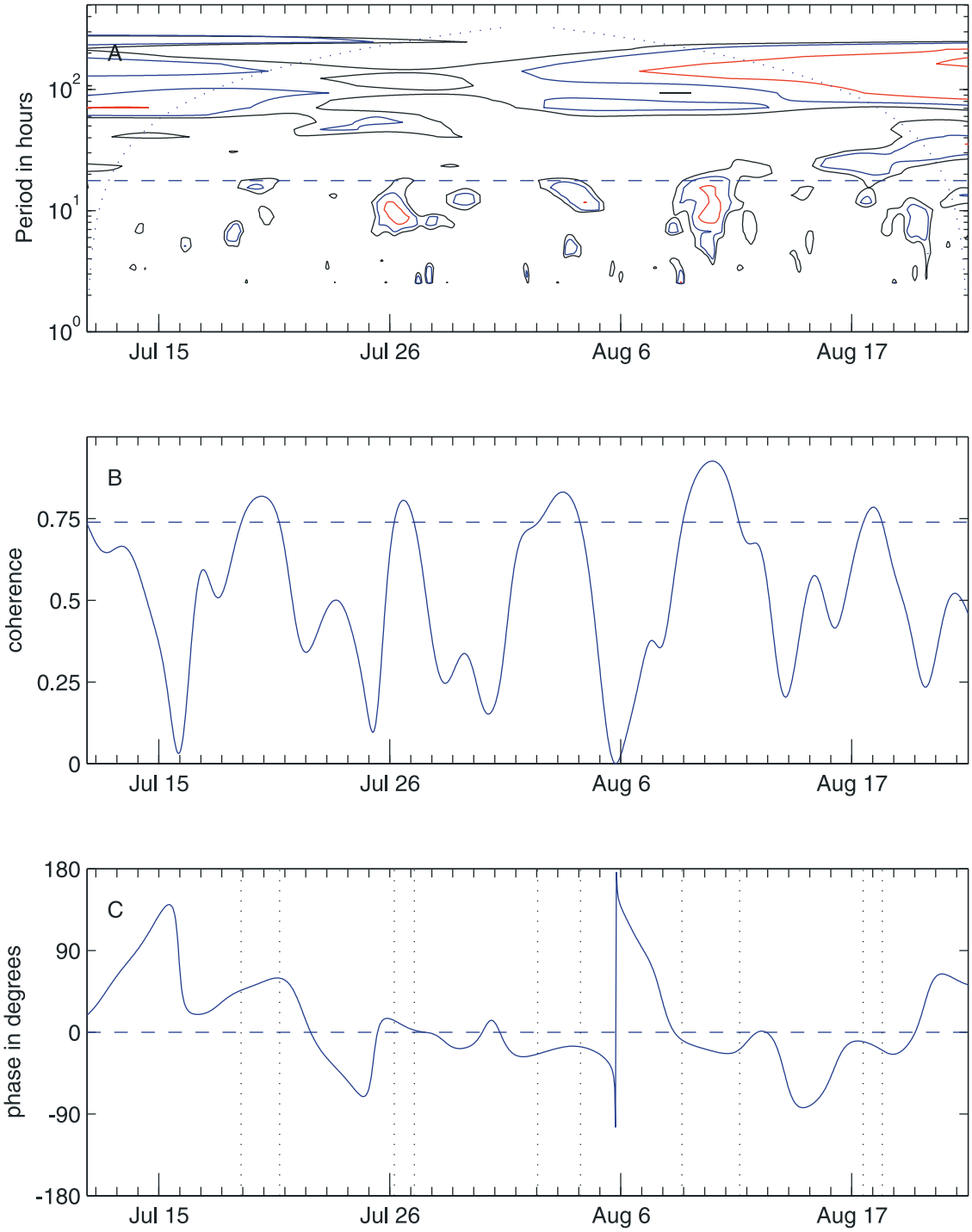

Figure 8. (a) Wavelet cross coherence for the beam attenuations at 1 and 7 mab. The black contour is the value at which the coherence is significantly different from zero at the 95% confidence level (0.74), the blue contour is 0.85, and the red contour is 0.95. The horizontal line is the inertial period (17.6 hours). The dotted curved lines are the cone of influence. (b) The cross coherence at the inertial period. The horizontal dashed line is the value above which the coherence is significantly different from zero at the 95% confidence level. (c) The phase angle. The vertical dotted lines mark the periods where the coherence is significantly different from zero. A negative value means that the 1 mab attenuation lags the 7 mab attenuation.

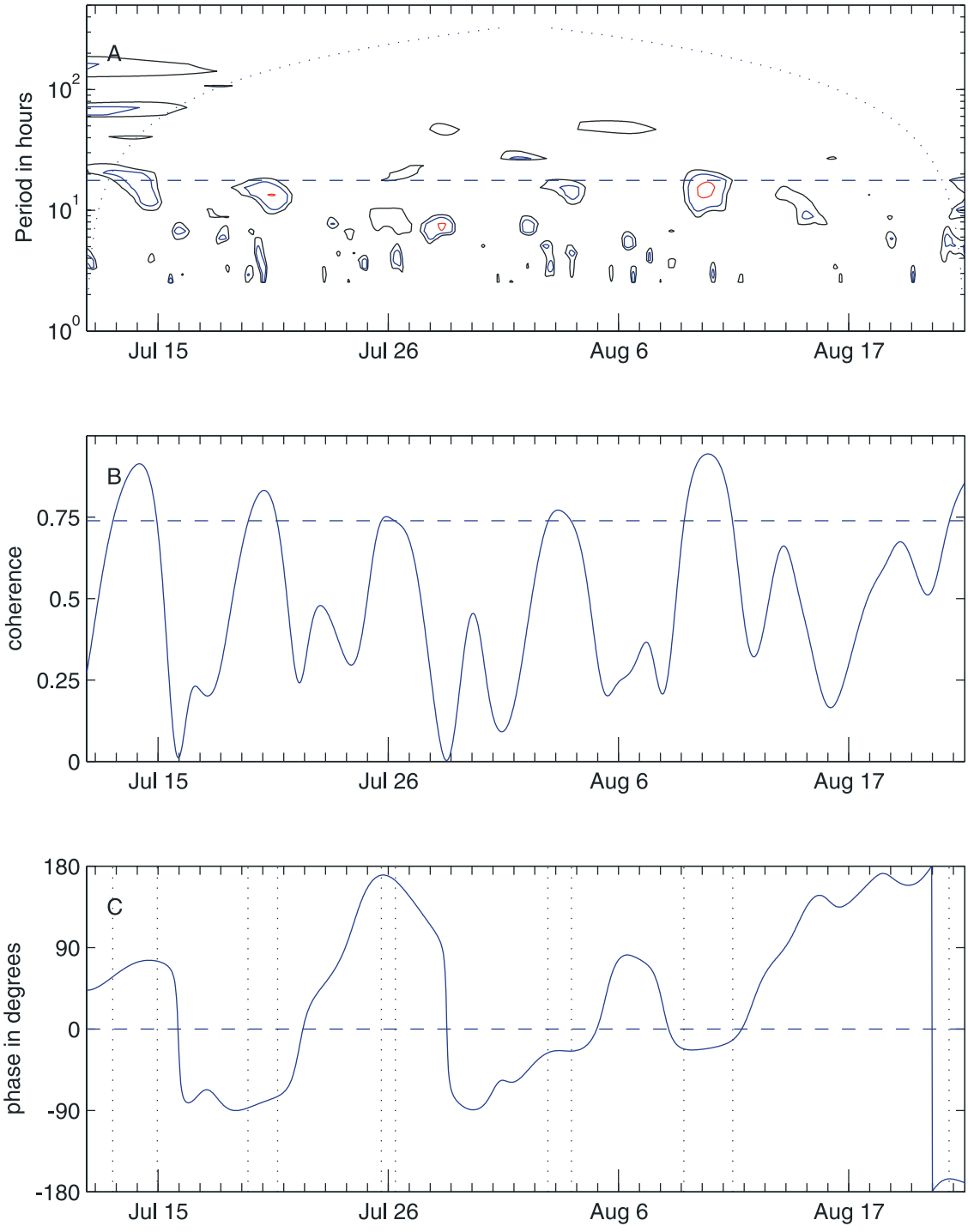

Figure 9. (a) Wavelet cross coherence for the cross-shore velocity and beam attenuations at 1 mab. The black contour is the value at which the coherence is significantly different from zero at the 95% confidence level (0.74), the blue contour is 0.85, and the red contour is 0.95. The horizontal line is the inertial period (17.6 hours). The dotted curved lines are the cone of influence. (b) The cross coherence at the inertial period. The horizontal dashed line is the value above which the coherence is significantly different from zero at the 95% confidence level. (c) The phase angle. The vertical dotted lines mark the periods where the coherence is significantly different from zero. A negative value means that the cross-shore velocity lags the attenuation.

Table 2. Periods of High Wavelet Cross Coherence Between the 1 mab Attenuation and the Cross-Shore Velocity at M27, the Wavelet Energies of the 1 mab Cross-Shore Velocity and 1 mab Attenuation, and the Phase Angle Between the Two Parameters[a]

Dates	Cross Coherence Between 1 mab Cross-Shore Velocity and 1 mab Attenuation	Energy Of 1 mab Bac	Energy of 1 mab Cross-Shore Velocity	Phase Angle Between 1 mab Cross-Shore Velocity and 1 mab Attenuation	Phase Angle Between 1 mab bac and 17 mab bac
July 13–15	X	X	X	60–90°	180°
July 19–21	X	X	X	−80°	10°
July 25	X	–	X	170°	180°
August 2–3	X	X	X	−30°	−30°
August 9–11	X	X	X	−30°	−30°
August 22	X	–	X	−170°	–

[a]Crosses indicates that the value is significantly different from zero; dashes indicate that the parameter is not significantly different from zero. A negative phase angle means that the first parameter lags the second.

did occur at M27, it appears that the appropriate conditions are related to the occurrence of upwelling events, which temporarily diminish the magnitude of the alongshore currents [*Rao and Murthy*, 2001]. This allows the onshore movement of bottom water, which may then in turn generate the internal waves responsible for the resuspension of the bottom material. *Hawley and Muzzi* [2003] also observed an increase in the thickness of the bnl during two upwelling events at a station close to M27, but were unable to identify the process responsible for the increase.

[27] If local resuspension does supply material to the bnl, then the material suspended in the water column should be similar to that on the bottom, but only a few studies have analyzed the chemical and mineralogic composition of material suspended in the bnl in the Great Lakes. *Eadie et al.* [1984] and *Robbins and Eadie* [1991] both found that the chemical composition of material collected in near-bottom sediment traps closely resembled that collected from the lake bottom, but *Harrsch and Rea* [1982] and *Mudroch and Mudroch* [1992] found that suspended sediment collected from water samples contained a much higher abundance of biologic material than did the surface sediments. This discrepancy may be at least partly due to the fact that water samples and sediment traps preferentially collect different types of material. Sediment traps tend to collect larger, more quickly settling particles, while material collected from water samples is biased toward smaller, more slowly settling material. Radiometric data [*Robbins and Eadie*, 1991] also shows that near-bottom trap material is derived primarily from bottom sediments, but the composition of material in the bnl undoubtedly varies with time and location.

[28] Profiles made during the winter [*Hawley and Lee*, 1999] and spring (N. Hawley, unpublished data) show that the bnl occurs intermittently during the unstratified period, but as the thermal bar moves offshore and the lake becomes stratified, a persistent bnl becomes increasingly well-developed. Both the thickness of the bnl and the amount of material in suspension varied during the summer, but the layer was always present at both M27 and M19, and was present at M24 whenever the water was stratified. Later in the year, as the water started to cool and vertical mixing became more intense, the nepheloid layers disappeared. Thus the development and decay of the nepheloid layers follows the thermal cycle of the lakes to a large degree, although storms during the unstratified period create a temporary bnl.

5. Conclusions

[29] The observations clearly show that near-inertial internal waves have a significant effect on the vertical distribution of suspended material in Lake Michigan during the stratified period. Although the precise mechanisms are still unknown, both the thickness and the distribution of suspended material within the bnl vary with the same period as the near-inertial waves in the lake. Unfortunately, it is not possible to determine if these episodes are caused by near-inertial waves or by shorter-period internal waves. When the changes in bac due to these internal waves are compared to those due to upwelling and downwelling events, it is clear that the longer-term processes are at least as important in determining the total amount of suspended sediment, and are also responsible for creating the conditions where internal waves can cause (either directly or indirectly) sediment resuspension. More extensive measurements will be needed before the effect of internal waves on the bnl will be fully understood.

Table 3. Periods of High Wavelet Cross Coherence Between the 1 mab Attenuation and the Cross-Shore Velocity at M24, the Wavelet Energies of the 1 mab Attenuation and the 1 mab Cross-Shore Velocity, and the Phase Angle Between the Two Parameters[a]

Dates	Cross Coherence Between 1 mab Cross-Shore Velocity and 1 mab Attenuation	Energy Of 1 mab Bac	Energy of 1 mab Cross-Shore Velocity	Phase Angle Between 1 mab Cross-Shore Velocity and 1 mab Attenuation	Phase Angle Between 1 mab Temperature and 1 mab Attenuation
July 12–13	X	X	X	80°	180°
July 18–20	X	X	X	90°	180°
August 4	X	X	X	90°	180°
August 6–9	X	X[b]	X	90°	180°
August 18–19	X	–	X	70°	180°

[a]Crosses indicate that the value is significantly different from zero; dashes indicate that the parameter is not significantly different from zero.
[b]August 6 only.

[30] The use of wavelets has considerable advantages over more traditional time series techniques since wavelets allow the data to be examined as a function of both time and period (or frequency). This allowed the identification of intervals within the deployment where changes in bac showed a consistent relationship to changes in other parameters. As in more traditional analyses, the fact that data were only collected at specified elevations makes the analysis more complex since only intervals when changes occurred at those specific elevations can be evaluated. Use of an in situ vertical profiler would allow data to be collected throughout the water column at regular intervals. Such data would almost certainly be easier to analyze and would allow the resolution of some of the questions that remain unanswered by this study.

[31] **Acknowledgments.** Thanks go the crew of the RV *Shenehon* and to Andy Winkelman and Chang-Hee Lee for their assistance with field operations. The Marine Instrumentation Laboratory of the Great Lakes Environmental Research Laboratory prepared and calibrated the sensors. Weather data were supplied by Clyde Sweet. Conversations with Gerry Miller and Dave Schwab helped in understanding the properties of internal waves in the lake. Wavelet power spectra software was provided by C. Torrence and G. Compo, and is available at http://paos.colorado.edu/research/wavelets. Software and advice for the wavelet cross-coherence calculations was kindly provided by C. Torrence. The comments and suggestions of two anonymous reviewers are gratefully acknowledged. This work was supported by the Environmental Protection Agency's Lake Michigan Mass Balance Study under interagency agreement DW131671701. This is GLERL contribution 1300.

References

Baker, J. E., and S. J. Eisenreich (1989), PCBs and PAHs as tracers of particulate dynamics in large lakes, *J. Great Lakes Res.*, *15*, 84–103.

Bogucki, D., T. Dickey, and L. G. Redekopp (1997), Sediment resuspension and mixing by resonantly generated internal solitary waves, *J. Phys. Oceanogr.*, *27*, 1181–1196.

Cacchione, D. A., and D. E. Drake (1986), Nepheloid layers and internal waves over continental shelves and slopes, *Geo Mar. Lett.*, *6*, 147–152.

Chambers, R. L., and B. J. Eadie (1981), Nepheloid and suspended particulate matter in southeastern Lake Michigan, *Sedimentology*, *28*, 439–447.

Eadie, B. J., R. L. Chambers, W. S. Gardner, and G. L. Bell (1984), Sediment trap studies in Lake Michigan: Resuspension and chemical fluxes in the southern basin, *J. Great Lakes Res.*, *10*, 307–321.

Halfman, B. M., and T. C. Johnson (1989), Surface and benthic nepheloid layers in the western arm of Lake Superior, 1983, *J. Great Lakes Res.*, *15*, 15–25.

Harrsch, E. C., and D. K. Rea (1982), Composition and distribution of suspended sediments in Lake Michigan during summer stratification, *Environ. Geol.*, *4*, 87–98.

Hawley, N. (2003), Observations of intermediate and benthic nepheloid layers in southern Lake Michigan during the summer of 1995, *NOAA Tech. Memo. GLERL-124*, 30 pp.

Hawley, N., and C.-H. Lee (1999), Sediment resuspension and transport in Lake Michigan during the unstratified period, *Sedimentology*, *46*, 791–805.

Hawley, N., and B. M. Lesht (1995), Does local resuspension maintain the benthic boundary layer in Lake Michigan?, *J. Sediment. Res., Sect. A*, *65*, 69–76.

Hawley, N., and C. R. Murthy (1995), The response of the benthic nepheloid layer to a downwelling event, *J. Great Lakes Res.*, *21*, 641–651.

Hawley, N., and R. W. Muzzi (2003), Observations of nepheloid layers made with an autonomous vertical profiler, *J. Great Lakes Res.*, *29*, 124–133.

Hawley, N., and J. E. Zyren (1990), Transparency calibration for Lake St. Clair and Lake Michigan, *J. Great Lakes Res.*, *16*, 113–120.

Jenkins, G. M., and D. G. Watts (1969), *Spectral Analysis and its Applications*, 525 pp., Holden-Day, Boca Raton, Fla.

Johnson, D. R., A. Weidemann, and W. S. Pegau (2001), Internal tidal bores and bottom nepheloid layers, *Cont. Shelf Res.*, *21*, 1473–1484.

Lee, C.-H., and N. Hawley (1998), The response of suspended particulate material to upwelling and downwelling events in southern Lake Michigan, *J. Sediment. Res.*, *68*, 819–831.

Li, M. Z., and C. L. Amos (2001), SEDTRANS96: The upgraded and better calibrated sediment-transport model for continental shelves, *Comput. Geosci.*, *27*, 619–645.

Liu, P. C., and G. S. Miller (1996), Wavelet transform and ocean current data analysis, *J. Atmos. Oceanic Technol.*, *13*, 1090–1099.

McCave, I. N. (1986), Local and global aspects of the bottom nepheloid layer in the world ocean, *Neth. J. Sea Res.*, *20*, 167–181.

Meyers, S. D., B. G. Kelly, and J. J. O'Brien (1993), An introduction to wavelet analysis in oceanography and meteorology with applications to the dispersion of Yanai waves, *Mon. Weather Rev.*, *121*, 2858–2866.

Mortimer, C. H. (1980), Inertial motion and related internal waves in Lake Michigan and Lake Ontario as responses to impulsive wind stresses, *Spec. Rep. 37*, 192 pp., Cent. for Great Lakes Stud., Milwaukee, Wis.

Mortimer, C. H., D. C. McNaught, and K. M. Stewart (1968), Short internal waves near their high-frequency limit in central Lake Michigan, paper presented at 11th Conference on Great Lakes Research, Int. Assoc. of Great Lakes Res., Ann Arbor, Mich.

Mudroch, A., and P. Mudroch (1992), Geochemical composition of the nepheloid layer in Lake Ontario, *J. Great Lakes Res.*, *18*, 132–153.

Murthy, C. R., and D. S. Dunbar (1981), Structure of the coastal boundary layer of the Great Lakes, *J. Phys. Oceanogr.*, *11*, 1567–1577.

Puig, P., A. Palanques, and J. Guillén (2001), Near bottom suspended sediment variability caused by storms and near inertial internal waves on the Ebro mid continental shelf (NW Mediterranean), *Mar. Geol.*, *178*, 81–93.

Rao, Y. R., and C. R. Murthy (2001), Nearshore currents and turbulent exchange processes during upwelling and downwelling events in Lake Ontario, *J. Geophys. Res.*, *106*, 2667–2678.

Ribbe, J., and P. E. Holloway (2001), A model of suspended sediment transport by internal tides, *Cont. Shelf Res.*, *21*, 395–422.

Robbins, J. A., and B. J. Eadie (1991), Seasonal cycling of trace elements ^{137}Cs, ^{7}Be, and $^{239+240}$Pu in Lake Michigan, *J. Geophys. Res.*, *96*, 17,081–17,104.

Rosa, F. (1985), Sedimentation and sediment resuspension in Lake Ontario, *J. Great Lakes Res.*, *11*, 13–25.

Sandilands, R. G., and A. Mudroch (1983), Nepheloid layer in Lake Ontario, *J. Great Lakes Res.*, *9*, 190–200.

Sly, P. G. (1994), Sedimentary processes in lakes, in *Sediment Transport and Depositional Processes*, edited by K. Pye, pp. 157-191, Blackwell Sci., Malden, Mass.

Torrence, C., and G. P. Compo (1998), A practical guide to wavelet analysis, *Bull. Am. Meteorol. Soc.*, *79*, 61–78.

Torrence, C., and P. J. Webster (1999), Interdecadal changes in the ENSO-monsoon system, *J. Clim.*, *12*, 2679–2690.

Wang, B. J., D. J. Bogucki, and L. G. Redekopp (2001), Internal solitary waves in a structured thermocline with implications for resuspension and the formation of thin particle layers, *J. Geophys. Res.*, *106*, 9565–9585.

Weng, H. Y., and K. M. Lau (1994), Wavelets, period doubling and time-frequency localization with application to organization of convection over the tropical western Pacific, *J. Atmos. Res.*, *51*, 2523–2541.

N. Hawley, Great Lakes Environmental Research Laboratory, 2205 Commonwealth Boulevard, Ann Arbor, MI 48105, USA. (nathan.hawley@noaa.gov)